742–755 *Nucleic Acids Research, 2008, Vol. 36, No. 3* *Published online 15 December 2007*
doi:10.1093/nar/gkm1092

Oxidation of single-stranded oligonucleotides by carbonate radical anions: generating intrastrand cross-links between guanine and thymine bases separated by cytosines

Conor Crean, Yuriy Uvaydov, Nicholas E. Geacintov and Vladimir Shafirovich*

Chemistry Department and Radiation and Solid State Laboratory, 31 Washington Place, New York University, New York, NY 10003-5180, USA

Received November 1, 2007; Revised and Accepted November 21, 2007

ABSTRACT

The carbonate radical anion is a biologically important one-electron oxidant that can directly abstract an electron from guanine, the most easily oxidizable DNA base. Oxidation of the 5′-d(CCTACGCTACC) sequence by photochemically generated $CO_3^{\bullet-}$ radicals in low steady-state concentrations relevant to biological processes results in the formation of spiroiminodihydantoin diastereomers and a previously unknown lesion. The latter was excised from the oxidized oligonucleotides by enzymatic digestion with nuclease P1 and alkaline phosphatase and identified by LC-MS/MS as an unusual intrastrand cross-link between guanine and thymine. In order to further characterize the structure of this lesion, 5′-d(GpCpT) was exposed to $CO_3^{\bullet-}$ radicals, and the cyclic nature of the 5′-d(G*pCpT*) cross-link in which the guanine C8-atom is bound to the thymine N3-atom was confirmed by LC-MS/MS, 1D and 2D NMR studies. The effect of bridging C bases on the cross-link formation was studied in the series of 5′-d(GpC$_n$pT) and 5′-d(TpC$_n$pG) sequences with $n = 0$, 1, 2 and 3. Formation of the G*-T* cross-links is most efficient in the case of 5′-d(GpCpT). Cross-link formation ($n = 0$) was also observed in double-stranded DNA molecules derived from the self-complementary 5′-d(TTACGTACGTAA) sequence following exposure to $CO_3^{\bullet-}$ radicals and enzymatic excision of the 5′-d(G*pT*) product.

INTRODUCTION

Interest in oxidative chemistry of carbonate radical anion, $CO_3^{\bullet-}$ has significantly grown within the last decade due to its important role in inflammatory processes (1,2). Persistent oxidative stress developed in response to inflammation in tissues is associated with overproduction of nitric oxide and superoxide radical anions that rapidly combine to form peroxynitrite (3). In cellular environments, the major mode of reaction of peroxynitrite (4–6) is the formation of a complex with CO_2 that decomposes rapidly to the oxidizing species, $CO_3^{\bullet-}$ and $^{\bullet}NO_2$ radicals (7,8). Only $CO_3^{\bullet-}$ radical can directly abstract an electron from guanine, the most easily oxidizable normal DNA base (9). This one-electron abstraction triggers a cascade of subsequent chemical reactions that yields stable oxidatively modified guanine (1,2). In previous work (10–12), we generated $CO_3^{\bullet-}$ radicals by a 308-nm excimer laser pulse-induced photochemical dissociation of peroxodisulfate anions to sulfate radical anions that subsequently oxidize bicarbonate anions to yield $CO_3^{\bullet-}$ radicals. The mechanisms of oxidation of 2′-deoxyoligonucleotides were studied by monitoring the transient absorbances of guanine and carbonate radicals, and by employing analytical and chemical methods to isolate and identify the chemical end products. Under these conditions, $CO_3^{\bullet-}$ radicals were generated in high concentrations and it was found that a consecutive four-electron oxidation of guanine yields, predominantly, the diastereomeric spiroiminodihydantoin (Sp) lesions (Figure 1).

In this work, we explored the oxidation of the 5′-d(CCTACGCTACC) sequence by $CO_3^{\bullet-}$ radicals generated by continuous illumination methods that generate low steady-state concentrations of carbonate radicals that are more relevant to biological conditions. The chemical end products of these oxidative processes were isolated by anion-exchange HPLC. In addition to the two diastereomeric Sp lesions found previously under conditions of laser pulse excitation that yields much higher transient concentrations of $CO_3^{\bullet-}$ radicals, a novel oxidatively generated lesion was found that was not observed previously (13,14). Using enzymatic digestion of the irradiated oligonucleotide followed by LC-MS/MS

*To whom correspondence should be addressed. Tel: +1 212 998 8456; Fax: +1 212 998 8421; Email: vs5@nyu.edu

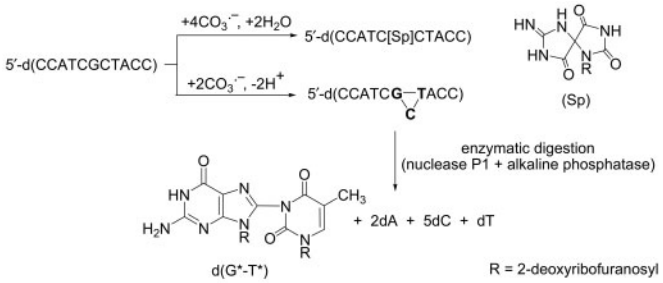

Figure 1. Lesions derived from the oxidation of single-stranded oligonucleotides by carbonate radical anions.

analysis of the digestion products, an excision fragment was found that has a mass smaller by 2 Da than the combined masses of dG and dT. The structure of this d(G*-T*) dimer is unusual because G and T are not adjacent to one another in the oligonucleotide. To gain further insights into the precursor of the enzymatic d(G*-T*) excision product, the trinucleotide 5′-d(GpCpT) was subjected to the same oxidation protocol as the oligonucleotide and the structure of the trinucleotide oxidation product was investigated by LC-MS/MS, 1D and 2D NMR methods. A cross-linked product, 5′-d(G*pCpT*) that has a covalent bond between the C8-atom of guanine and the N3-atom of thymine was found that has the same characteristics as the corresponding product excised from the 11-mer oligonucleotide. The cross-linked product generated by oxidation with $CO_3^{\bullet-}$ radicals (Figure 1) differs from the cross-links between adjoining G and T bases produced by ionizing radiation in deoxygenated solutions that involve a covalent bond between the C8-atom of guanine and the C-atom of the methyl group in thymine (15–24). Here, we investigated the effects of bridging C bases between G and T on the efficiency of the cross-link formation in a series of the oligonucleotide sequences 5′-d(GpC$_n$pT) and 5′-d(TpC$_n$pC) with $n = 0$, 1, 2 and 3, and cross-linking in a 12-mer duplex derived from the self-complementary 5′-d(TTACGTACGTAA) sequence.

MATERIALS AND METHODS

Materials

All chemicals (analytical grade) were used as received. Snake venom phosphodiesterase was purchased from Pharmacia (Piscataway, NJ, USA); calf spleen phosphodiesterase, nuclease P1 and alkaline phosphatase were from Sigma Chemical (St Louis, MO, USA). The oligonucleotides were purchased from Sigma Genosys (Woodlands, TX, USA), purified and desalted using reversed-phase HPLC. The integrity and composition of the oligonucleotides were confirmed by MALDI-TOF/MS and LC-MS/MS techniques.

Photochemical oxidation of oligonucleotides

Oligonucleotides (10 nmol) were dissolved in 1 ml of air-equilibrated solutions containing 300 mM $NaHCO_3$ and 10 mM $Na_2S_2O_8$ and the pH was adjusted to 7.5 with 1 M NaH_2PO_4. The solutions were irradiated with light from a 100-W high-pressure Xenon lamp that was reflected from a dichroic mirror with the reflectance in the 300–340-nm spectral range. In the experiments with riboflavin (RF) (~15 μM), the solutions were irradiated by 350–390 nm light from the same Xenon lamp and this wavelength range was isolated by means of an appropriate dichroic mirror. The energy incident on the sample was ~100 mW/cm^2 and the irradiation time was varied from 10 to 30 s depending on the sequence. After irradiation, the sample was immediately desalted by reversed-phase HPLC, concentrated and subjected to HPLC analysis.

Separation by anion-exchange HPLC methods

The photochemical reaction products were separated using an Agilent 1200 Series LC system (quaternary LC pump with degasser, thermostated column compartments, and diode array detector) equipped with an analytical (250 × 4 mm i.d.) anion-exchange DNAPac PA-100 column (Dionex, Sunnyvale, CA, USA). Typically, the anion-exchange HPLC separations of the oxidized oligonucleotides were performed employing a 10–90% linear gradient of solvent B (10% acetonitrile and 90% 1.5 M ammonium acetate) in solvent A (10% acetonitrile and 90% water) for 30 min at a flow rate of 1 ml/min (25,26). The trinucleotide products were separated using an isocratic mobile phase (90% solvent A and 10% solvent B) at a flow rate of 1 ml/min. The purified adducts were desalted by reversed-phase HPLC using the following mobile phases: 5 mM sodium phosphate (pH 7.5) (10 min), deionized water (10 min) and 50% methanol in water (15 min). The desalted samples were concentrated under vacuum and subjected to LC-MS/MS and NMR analysis.

Enzymatic and chemical digestion of oligonucleotides

The cross-linked oligonucleotide adducts (10 nmol) were digested with nuclease P1 (2 U) in 35 μl of 30 mM acetate buffer (pH 5.2) overnight at 37°C; following digestion, the samples were treated with 2 U of alkaline phosphatase in a Tris–HCl (~100 mM) buffer solution (pH 8.2) for 1 h at 37°C. The incubation mixtures were passed through a Millipore centrifugal filter to remove the enzymes. The nucleosides were separated by reversed-phase HPLC using a 0–40% linear gradient of acetonitrile in 20 mM ammonium acetate for 60 min at a flow rate of 1 ml/min and subjected to LC-MS/MS analysis.

Chemical hydrolysis of the cross-linked products was performed using a commercially available solution of hydrogen fluoride (~70%) in pyridine (HF/Pyr) as previously described (27). The dry, cross-linked product (1–3 nmol) generated by the oxidation of 5′-d(GpCpT) was treated in a plastic vial with 50 μl of HF/Pyr at 37°C for 30 min. The reaction mixture was diluted with 1 ml of water and neutralized by vigorous agitation with 80 mg of $CaCO_3$. The insoluble inorganic salts were removed by centrifugation. The sample was evaporated to dryness and traces of pyridine were removed by repeated lyophilization. The final aqueous solution (~20 μl) was passed through a Millipore centrifugal filter and diluted by water up to ~100 μl prior to HPLC separation. The hydrolysis

products were isolated on a (100 × 3 mm i.d.) Hypercarb column (Thermo-Hypersil-Keystone, Bellefonte, PA) employing 0–90% gradient of acetonitrile in 2-mM ammonium acetate for 40 min at a flow rate 1 ml/min, lyophilized and subjected to LC-MS/MS analysis.

LC-MS/MS experiments

Analysis of the photoproducts was performed with an Agilent 1100 Series capillary LC/MSD Ion Trap XCT mass spectrometer equipped with an electrospray ion source (ion trap conditions: ESI ionization, nebulizing gas 40 psi, drying gas 8 l/min, drying gas temperature 350°C, acquisition range m/z 80–2000, target mass set to molecular ion of interest, manual MS/MS, fragmentation amplitude 1.0 V, fragmentation time 10 ms, fragmentation width 2 Da). The end products derived from oxidation of 5′-d(GpC$_n$pT) sequences (n = 0, 1) were analyzed using 1–8 µl injection of the sample solution in a narrowbore (50 × 1 mm i. d.) Zorbax SB-C8 column and elution with an isocratic mixture (50% acetonitrile in water with 0.1% formic acid) at a flow rate of 0.2 ml/min. The mass spectra were recorded in the positive mode. The spectrometer was tuned to maximum sensitivity using a direct infusion of the d(GpC$_n$pT) standard solutions. The oxidatively modified 4–11mer oligonucleotides were analyzed using 1–8 µl loop injection elution with an isocratic mixture (50% acetonitrile in 15 mM imidazole) at a flow rate of 0.2 ml/min. The negative multiply charged ion spectra were deconvoluted using Agilent Data Analysis 5.2 software.

NMR spectra of the oligonucleotide irradiation products

The 1D ^{1}H and ^{13}C spectra, and 2D DQF-COSY (double quantum filtered) and magnitude COSY (correlation spectroscopy), HSQC (heteronuclear single quantum correlation), HMBC (heteronuclear multiple bond correlation) and NOESY (nuclear Overhauser effect spectroscopy) spectra were recorded in D_2O using 400 MHz and 500 MHz Bruker NMR instruments and a sample concentration of 1.3 mM. The chemical shifts are given relative to sodium 2,2-dimethyl-2-silapentane-5-sulfonate (DSS).

RESULTS

Generation and identification of the oligonucleotide reaction products

The $CO_3^{\bullet-}$ radicals were generated by the photochemical method used in our previous experiments (10–12). This method involves the photodissociation of peroxodisulfate to sulfate radical anions, followed by the one-electron oxidation of HCO_3^- anions with $SO_4^{\bullet-}$ radicals. The reaction products derived from the reactions of the single-stranded oligonucleotide, 5′-d(CCATCGCTACC) with the photochemically generated $CO_3^{\bullet-}$ radicals were separated from the unmodified oligonucleotides by anion-exchange HPLC methods (Figure 2A). The products were collected, desalted and subjected to analysis by LC-MS/MS. The mass spectra were recorded in the negative mode and deconvoluted. The unmodified sequence eluted after 16.7 min (mass, M: 3237.2),

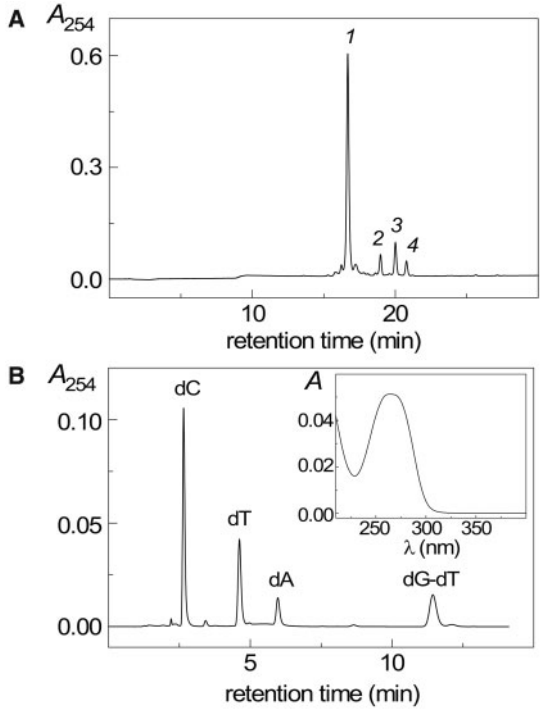

Figure 2. (**A**) Anion-exchange HPLC elution profile of the end products derived from the oxidation of the single-stranded oligonucleotide, 5′-d(CCATCGCTACC) by $CO_3^{\bullet-}$ radicals. The 5′-d(CCATCGCTACC) sequence (0.01 mM) was dissolved in air-equilibrated buffer solution (pH 7.5) containing 300 mM $NaHCO_3$ and 10 mM $Na_2S_2O_8$, and was irradiated for 10 s. HPLC elution conditions (detection at 254 nm): 10–90% linear gradient of solvent B (10% acetonitrile and 90% 1.5 M ammonium acetate) in solvent A (10% acetonitrile and 90% water) for 30 min at a flow rate of 1 ml/min. The intact sequence elutes at 16.7 min (i), the unknown modified oligonucleotide with mass M–2 elutes at 19.0 min (ii), the oligonucleotides with the single G converted to the spiroiminodihydantoin lesions with the (+)-*R*-Sp (iii) and (−)-*S*-Sp (iv) configurations elute at 20 min, and 20.8 min, respectively. The absolute configurations of the Sp lesions were determined as described by Durandin *et al.* (28). (**B**) Reversed-phase HPLC elution profile of the products generated by the enzymatic digestion of the M–2 oligonucleotide adduct. HPLC elution conditions (detection at 254 nm): 0–40% linear gradient of acetonitrile in 20 mM ammonium acetate for 30 min at a flow rate of 1 ml/min. The dC nucleoside elutes at 2.7 min, dT at 4.6 min, dA at 6.0 min,and the d(G*-T*) product with mass of 507.3 elutes at 11.4 min. The inset shows the absorption spectrum of the concentrated fraction eluted at 11.4 min.

the sequences with diastereomeric spiroiminodihydantoin lesions at 20.0 and 20.8 min (M + 32: 3259.2) and a novel product eluted at 19.0 min (M-2: 3235.2) as shown in Figure 2A. The retention times of the fractions 3 and 4 containing the oligonucleotides with single Sp lesions instead of guanine were identical to those of the authentic standards containing the diastereomeric Sp lesions with (+)-*R* and (−)-*S* absolute configurations (11,28). Therefore, in the experiments described here, we focused on the identification of the M-2 adducts that eluted at 19.0 min (fraction 2 in Figure 2A).

The M-2 oligonucleotide adducts obtained in a series of photochemical experiments were combined, desalted and enzymatically digested by nuclease P1 and alkaline phosphatase; the digestion products were separated by

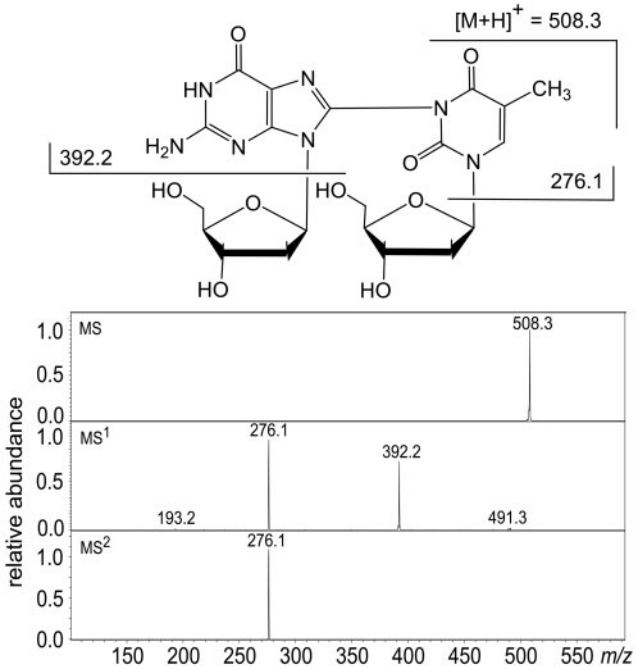

Figure 3. The positive ion spectra (MS/MS) of the d(G*-T*) product obtained by enzymatic digestion of the M–2 oligonucleotide adduct (product 2 in Figure 2A). MS spectrum of the molecular ion, $[M + H]^+$ at m/z 508.3. MS^1 product ion spectrum obtained by fragmentation of the molecular ion, $[M + H]^+$ at m/z 508.3. MS^2 product ion spectrum obtained by fragmentation of the ion, $[M + H - 116]^+$ at m/z 392.2.

reversed-phase HPLC (Figure 2B). The digestion product eluting at 11.4 min is characterized by a strong UV absorption band at 270 nm (inset in Figure 2B) indicating that this product contains aromatic nucleobases. The 11.4 min product was desalted, concentrated and subjected to LC-MS/MS analysis. The positive ion spectra (MS/MS) of this digestion product are shown in Figure 3. The molecular ion, $[M + H]^+$ is detected at m/z 508.3. Interestingly, the mass of the digestion product (507.3 Da) is equal to the combined masses of the dG and dT nucleosides minus 2 Da. A plausible structure of the digestion product is shown in Figure 3, and involves a covalent interstrand cross-link between the C8 position of dG and the N3-position of dT that requires the removal of two H atoms. This product lacks the nucleotide pdCp that normally separates the dG and dT in the 5′-d(CCATCGCTACC) sequence. This product is also very different from the intrastrand cross-linked lesions previously reported that involve chemical bonds between C8-G and methyl group of the adjacent T base (15–24).

To obtain insights into the structure of this unusual product, we analyzed the fragmentation patterns of the parent molecular ion, $[M + H]^+$ at m/z 508.3 (Figure 3). Fragmentation of $[M + H]^+$ occurs via the cleavage of the *N*-glycosidic bond with the concomitant transfer of a hydrogen atom from the sugar residue to the base (29–31). The signals detected at m/z 392.2 and m/z 276.1 correspond to the ions, $[M + H - 116]^+$ and $[M + H - 232]^+$, respectively, derived from the consecutive detachment of two sugar residues from $[M + H]^+$. The ion at m/z 276.1 is assigned to the G*-T* fragment and its mass is equal to the sum of the masses of G and T minus 2 Da. These results further suggest that the M-2 product derived from the oxidation of 5′-d(CCATCGCTACC) with $CO_3^{\bullet-}$ radicals contains an intrastrand cross-link between G and either 3′-T or 5′-T. This cross-linked product is resistant to digestion by the nuclease P1, although the nucleotide pdCp between the bases is removed by the combined action of nuclease P1 and alkaline phosphatase.

The 5′-d(CCATCGCTACC) sequence contains two isolated T bases, one positioned on the 5′- side and the other on the 3′-side of the central G that is initially oxidized by the carbonate radical (10). The site of the cross-link was identified by enzymatic digestion with phosphodiesterases followed by MALDI-TOF/MS analysis of the digestion products. The mass spectra recorded in the negative mode showed that digestion of the M-2 oligonucleotide adduct from the 3′-end by snake venom phosphodiesterase I stalls at base T_2 thus yielding the modified fragment 5′-d($CCAT_1CGCT_2$)*, which shows a signal at m/z 2342.2 after a prolonged digestion. In contrast, the fragment 5′-d($CGCT_2ACC$)* was detected at m/z 2038.2 when the digestion of the full modified 11-mer oligonucleotide with a mass of M-2 was digested from the 5′-end by bovine spleen phosphodiesterase II. The successful removal of the base T_1 by phosphodiesterase II indicates that the intrastrand cross-link involves reaction at T_2. The involvement of T_2 in cross-link formation was confirmed by treating 5′-^{32}P-labeled M-2 sequences with hot piperidine at 90°C for 30 min (32) and resolving the cleavage products using high-resolution denaturing polyacrylamide gel electrophoresis (data not shown). Cleavage was observed mostly at T_2 (~70%), although lesser extents of cleavage at the G (~7%) and T_1 (~9%) sites were also detected. These observations indicate that the base T_2 is damaged and that hot piperidine treatment generates the fragments 5′-^{32}P-d($CCAT_1CG^*C$) in which G* is only partially alkali-labile. The minor extent of cleavage at T_1 indicates that cross-linking at T_1 does not exceed ~9%.

In order to further elucidate the involvement of T on the 5′- and 3′-sides of the single guanine residue in the cross-linking reaction, we investigated the reactivities of the 5′-d(GpCpT) and 5′-d(TpCpG) sequences with $CO_3^{\bullet-}$ radicals. The cross-linked products, 5′-d(G*pCpT*) and 5′-d(T*pCpG*) derived from the oxidation of these trinucleotides (10 μM) were isolated by anion-exchange HPLC (Figure 4) and identified by LC-MS/MS analysis (Figure 5 and Figure S1 in Supplementary Data). In the case of 5′-d(GpCpT), ~1 nmol of 5′-d(G*pCpT*) and ~0.4 nmol of the diastereomeric Sp adducts were obtained (Figure 4A). In contrast, 0.2 nmole of 5′-d(T*pCpG*) and ~0.4 nmole of the Sp products were isolated after oxidation of 5′-d(TpCpG) (Figure 4B). These differences in yields of the cross-linked products indicate that the T on the 3′-side of G in 5′-d(GpCpT) is more reactive than the T on the 5′-side in 5′-d(TpCpG).

The positive ion spectra (MS/MS) of 5′-d(G*pCpT*) are shown in Figure 5. The mass of the cross-linked product with molecular ion, $[M + H]^+$ detected at m/z 859.1

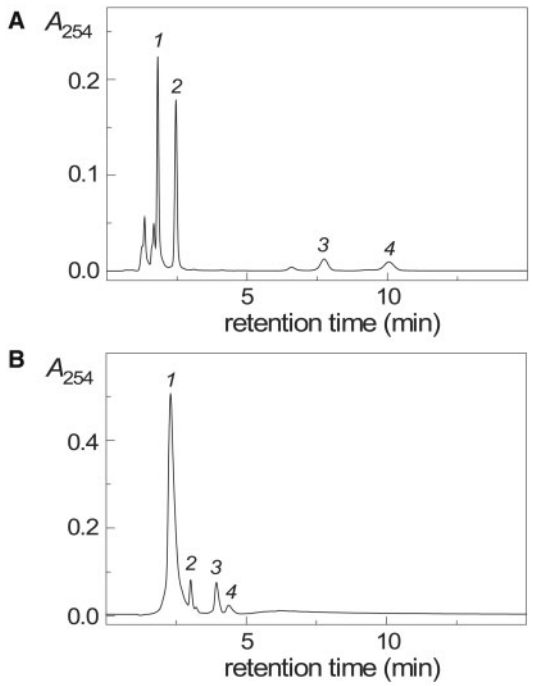

Figure 4. Anion-exchange HPLC elution profiles of the end-products derived from the oxidation of the 5′-d(GpCpT) and 5′-d(TpGpC) sequences by $CO_3^{\bullet-}$ radicals. The trinucleotides (0.01 mM) in air-equilibrated buffer solutions (pH 7.5) containing 300 mM $NaHCO_3$ and 10 mM $Na_2S_2O_8$ were irradiated for 10 s. HPLC elution conditions (detection at 254 nm): isocratic elution using 90% solvent A (10% acetonitrile and 90% water) and 10% solvent B (10% acetonitrile and 90% 1.5 M ammonium acetate) at a flow rate of 1 ml/min. (**A**) The intact 5′-d(GpCpT) elutes at 1.8 min (i), 5′-d(G*pCpT*) at 2.5 (ii), the (+)-*R*-Sp and (−)-*S*-Sp trinucleotides at 7.7 min (iii) and 10.0 min (iv), respectively. (**B**) The intact 5′-d(TpCpG) elutes at 2.3 min (i), 5′-d(T*pCpG*) at 3.0 (i), the (+)-*R*-Sp and (−)-*S*-Sp trinucleotides at 3.9 min (iii) and 4.4 min (iv), respectively.

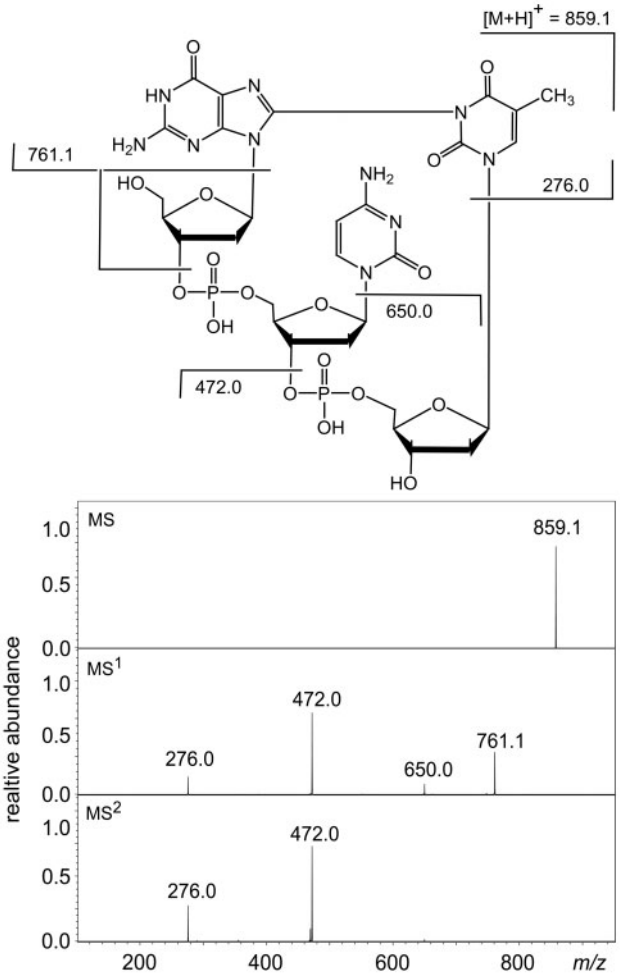

Figure 5. Positive ion spectra (MS/MS) of 5′-d(G*pCpT*). MS spectrum of the molecular ion, $[M + H]^+$ at m/z 859.1. MS^1 product ion spectrum obtained by fragmentation of the molecular ion, $[M + H]^+$ at m/z 859.1. MS^2 product ion spectrum obtained by fragmentation of the ion, $[M + H - 387]^+$ at m/z 472.0.

(Figure 5) is smaller by 2 Da than the mass of the unmodified 5′-d(GpCpT) observed at m/z 861.2. The fragmentation of $[M + H]^+$ occurs via typical pathways for protonated oligonucleotides involving cleavage of the *N*-glycosidic bond and the phosphodiester C3′–O3′ bond with the concomitant transfer of two hydrogens from the sugar residue to the base and phosphate (29–31). The ion, $[M + H - 98]^+$ arising from the fragmentation of $[M + H]^+$ associated with the release of a furan-type residue is detected at m/z 761.1. Further cleavage of $[M + H - 98]^+$ that releases cytosine, generates the ion $[M + H - 209]^+$ observed at m/z 650. The ions, $[M + H - 387]^+$ at m/z 472.0 and $[M + H - 583]^+$ at m/z 276.0 are derived from cleavage of the C3′–O3′ bond in $[M + H - 209]^+$ and the *N*-glycosidic bond in $[M + H - 387]^+$, respectively. The mass of $[M + H - 583]^+$ is identical to that of the ion at m/z 276.0 observed in the spectra of the d(G*-T*) dimer enzymatically excised from the 11mer product (Figure 3).

The molecular ion, $[M + H]^+$, derived from 5′-d(T*pCpG*) was detected at m/z 859.2 (Figure S1 in Supplementary Data), i.e. the mass of this cross-linked product is equal to that of 5′-d(G*pCpT*) (Figure 5). The fragmentation of $[M + H]^+$ produced from 5′-d(T*pCpG*) generates a series of ions, including the T*-G* ion, $[M + H - 583]^+$ detected at the characteristic m/z 276.0 setting (Figure S1). Thus, the LC-MS/MS results indicate that the oxidation of 5′-d(GpCpT) and 5′-d(TpCpG) sequences by $CO_3^{\bullet-}$ radicals yield the cyclic products with the identical masses in which G and T are linked to one another and are separated by a single C residue (Figures 5 and S1).

Acid hydrolysis of the cross-linked trinucleotide and LC-MS/MS analysis of the hydrolysis products

The positive ion spectra (MS/MS) show that the cross-linked products can be easily fragmented in our ion trap mass spectrometer to the level of a G*-T* dimer detected at m/z 276.2 (Figures 3, 5, 6, S1 and S2). However, attempts to further fragment this dimer failed because amounts of the daughter ions produced were too low for detection. To improve detection of the daughter ions, we attempted to decrease the number of fragmentation steps by a preliminary chemical hydrolysis of 5′-d(G*pCpT*) by

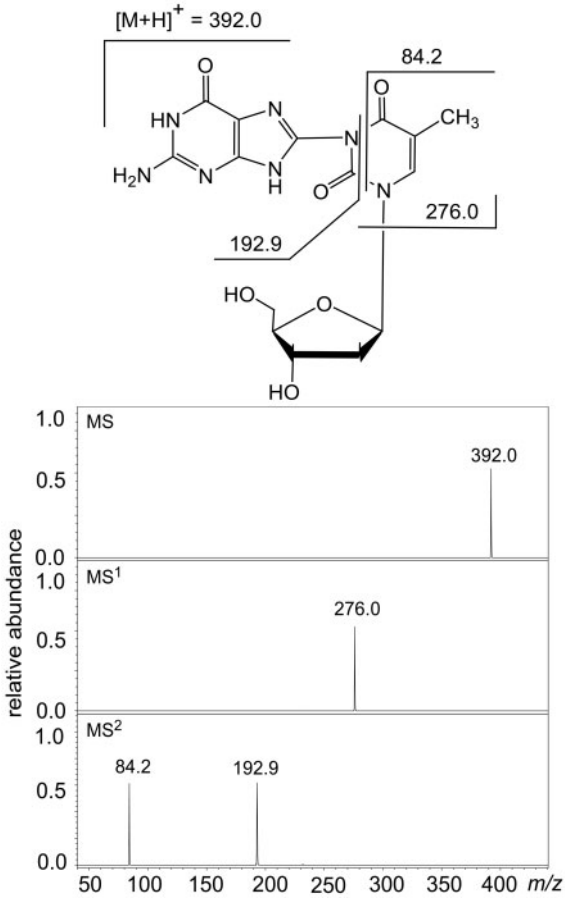

Figure 6. The positive ion spectra (MS/MS) of the cross-linked product obtained by hydrolysis of 5′-d(G*pCpT*) with HF/Pyr. MS spectrum of the molecular ion, $[M + H]^+$ at m/z 392.0. MS^1 product ion spectrum obtained by fragmentation of the molecular ion, $[M + H]^+$ at m/z 392.0. MS^2 product ion spectrum obtained by fragmentation of the ion, $[M + H - 116]^+$ at m/z 276.0.

hydrogen fluoride stabilized by pyridine (HF/Pyr). Cadet and co-workers showed that HF/Pyr treatment allows for the fast and quantitative release of oxidatively modified guanine (27) and thymine (33) bases from DNA at 37°C. After hydrolysis of 5′-d(G*pCpT*), the products were isolated by reversed-phase HPLC and subjected to LC-MS/MS analysis. The positive ion spectra of the main hydrolysis product are shown in Figure 6. The molecular ion, $[M + H]^+$ detected at m/z 392.0 corresponds to the G*-dT* dimer containing a single sugar residue. Since, the *N*-glycosidic bonds in pyrimidines are more stable to acid hydrolysis than the *N*-glycosidic bonds of purines (34,35), we propose that the sugar residue is linked to the T base rather than to the G base (Figure 6). Chemical hydrolysis of 5′-d(G*pCpT*) was also performed in 1 N HCl at 85°C for 1 h. The hydrolysis products were separated by reversed-phase HPLC and identified by LC-MS/MS analysis. The positive ion spectra of these products exhibit molecular ions, $[M + H]^+$ detected at m/z 392.0 and at m/z 276.0, which were assigned to the dimers with either a single sugar residue (G*-dT*) or without any sugar residue (G*-T*), respectively. However, the yields of these dimers produced by HCl hydrolysis were lower than in the case of HF/Pyr hydrolysis, most likely due to the formation of side products associated with the isomerization and anomerization of the thymine 2-deoxyribose residue that compete with hydrolysis of the *N*-glycosidic bond (36).

The fragmentation of the molecular ion, $[M + H]^+$ at m/z 392.0 (Figure 6) generates the ion, $[M + H - 116]^+$ at m/z 276.0 derived from the cleavage of the *N*-glycosidic bond with release of a sugar residue (29–31). Further fragmentation of $[M + H - 116]^+$ yields the daughter ions, $[M + H - 199]^+$ at m/z 192.9 and $[M + H - 208]^+$ at m/z 84.2 (Figure 6). We note that further fragmentation of these ions in our XCT ion trap produces only negligible amounts of daughter ions that could not be identified. The ions at m/z 192.9 and m/z 84.2 are derived from the cleavage of the N3–C4 and C2–N1 bonds of thymine (Figure 6); these are typical of the fragmentation of thymine derivatives (37). According to this mode of fragmentation, only the N3 or O2 atoms of thymine can be involved in the formation of a bond with the G base. However, Singer and co-workers (38) have shown that alkylation of the O2 atom of thymine greatly destabilizes the *N*-glycosidic bond, and in acid solutions (pH 1.5) the O2-alkylated thymidines undergo a rapid depyrimidination, followed by dealkylation. The O4-alkylated thymidine residues are also dealkylated under these conditions; however, depyrimidination does not occur because of the more stable *N*-glycosidic bonds in these thymidine derivatives. We expect that any cross-linked products containing the C8–O2 (or C8–O4) linkage would not have survived acid hydrolysis under our conditions. Therefore, we conclude that the cross-link occurs via a C8/G–N3/T bond rather than a C8/G–O/T linkage.

NMR characteristics of the cross-linked product derived from the oxidation of 5′-d(GpCpT)

The participation of the C8 atom of guanine in the cross-linked product is further supported by NMR data. The formation of a G*pT* cross-link (tandem lesion) in the tetranucleotide, d(CGTA) subjected to ionizing radiation in aqueous solution under anoxic conditions was first reported by Box *et al.* (15). Utilizing NMR methods they showed that the protons at the C8 position of G and a proton at the methyl group of T were absent, in contrast to the unirradiated controls, and concluded that the irradiation produced a cross-link involving a covalent bond between the C8 carbon atom of guanine and the carbon atom of the thymine methyl group. Unlike the cross-link in our 11-mer and trimer oligonucleotides that involve a covalent bond between G and T separated by C, the cross-linked product observed by Box *et al.* (15–19), Cadet *et al.* (20–22) and by Hong *et al.* (23,24), involved the adjacent G and T residues.

In order to further characterize the sites at the G and T residues that are involved in the formation of the covalent bond in the cross-linked product generated by the oxidation of the 5′-d(GpCpT) sequences with $CO_3^{\bullet-}$ radicals, we carried out extensive 1D and 2D NMR analysis. Initially, we compared the 1D proton NMR

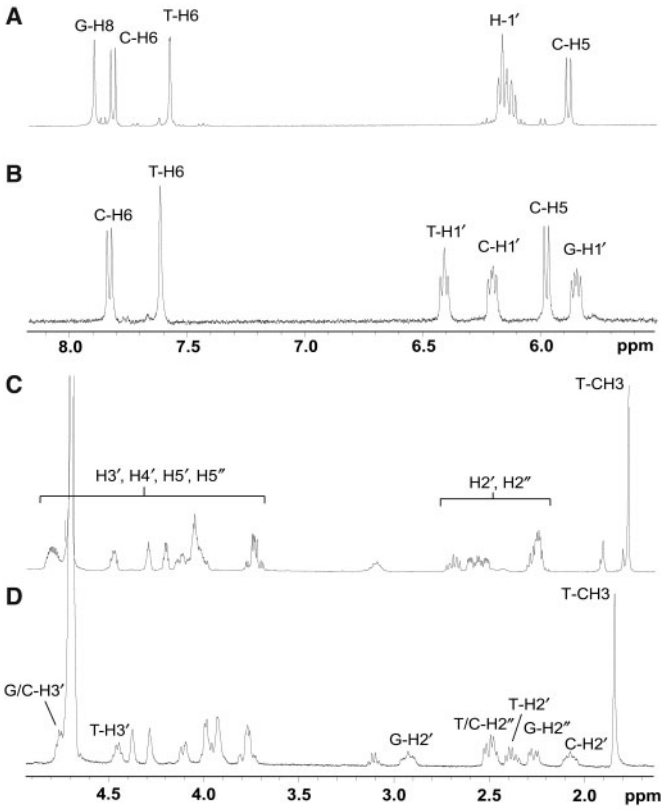

Figure 7. The 1D proton NMR spectra of the intact 5′-d(GpCpT) (**A** and **C**) and 5′-d(G*pCpT*) (**B** and **D**).

spectra of 5′-d(G*pCpT*) (product 2, Figure 4A) and the unirradiated, intact 5′-d(GpCpT) trinucleotide. These spectra were recorded in D_2O solutions where the resonances of the exchangeable imino protons are not detectable (Figure 7). Comparison of the 5.5–8.5 p.p.m. portions of the spectra clearly show that the guanine H8 proton is present in the spectrum of the intact sequence (Figure 7A), but is absent in the spectrum of the cross-linked product (Figure 7B). This is straightforward evidence that guanine in 5′-d(G*pCpT*) is linked to the T base via its C8 carbon atom.

The thymine H6 singlet is evident at 7.6 p.p.m. (Figure 7A and B), and the characteristic $-CH_3$ singlet due to the thymine methyl group is evident below 1.9 p.p.m. in the control as well as in the cross-linked trinucleotide (Figure 7C and D). This clearly suggests that the covalent bond in our cross-linked G-T fragment does not involve the thymine methyl group as in the G-T tandem lesions reported previously (15–19). It is noteworthy that the 2-deoxyribose H1′ protons appear as three distinct multiplets in 5′-d(G*pCpT*) as opposed to the overlapping multiplet in 5′-d(GpCpT). Also there is a distinct shift in the 2-deoxyribose H2′/H2″ signals in 5′-d(G*pCpT*) compared to the control. These differences allowed for the assignment of the majority of the proton (Table 1) and ^{13}C NMR resonances (Table 2) for the cross-linked 5′-d(G*pCpT*) oxidation product.

Examples of some of the assignments of ^{13}C resonances based on HSQC and HMBC correlation spectra are depicted in Figure 8A and B, respectively. The ^{1}H resonances corresponding to the 2-deoxyribose H4′, H5′, H5″ and their respective ^{13}C signals could not be unambiguously assigned. The process by which all the NMR signals were assigned (Tables 1 and 2) is described, and more complete 1D ^{13}C NMR, 2D COSY, HSQC and HMBC spectra are provided in Supplementary Data.

Table 1. ^{1}H NMR chemical shifts of 5′-d(G*pCpT*)

Thymine		Cytosine		Guanine	
T-CH_3	1.85	C-H5	5.96, 5.98	G-H1′	5.83–5.86
T-H6	7.61	C-H6	7.82, 7.84	G-H2′	2.89–2.92
T-H1′	6.3–6.4	C-H1′	6.18–6.22	G-H2″	2.24–2.29
T-H2′	2.34–2.41	C-H2′	2.07–2.09	G-H3′	4.74–4.77[a]
T-H2″	2.46–2.52[a]	C-H2″	2.46–2.52[a]	G-H4′	
T-H3′	4.44–4.46	C-H3′	4.74–4.77[a]	G-H5′	
T-H4′		C-H4′		G-H5″	
T-H5′		C-H5′			
T-H5″		C-H5″			

[a]Overlapping peaks.

Table 2. ^{13}C NMR chemical shifts of 5′-d(G*pCpT*)

Thymine		Cytosine		Guanine	
T-C2	153.69	C-C2	159.9	G-C2[a]	156.55
T-C4	167.16	C-C4	168.55	G-C4	153.84
T-C5	113.90	C-C5	98.90	G-C5[a]	118.09
T-C6	140.49	C-C6	143.6	G-C6[a]	161.27
T-CH_3	14.28	C-C1′	89.02	G-C8	137.5
T-C1′	86.86	C-C2′	41.87	G-C1′	87.65
T-C2′	39.77	C-C3′	79.80	G-C2′	39.57
T-C3′	71.89	C-C4′		G-C3′	79.00
T-C4′		C-C5′		G-C4′	
T-C5′				G-C5′	

[a]Assignments based on their expected positions in 2′-deoxyguanosine.

Effect of number of C residues separating G and T on the efficiency of cross-link formation

In the sequences, 5′-d(CCATCGCTACC) and 5′-d(GpCpT) that we studied, the G and T bases are separated by a single C residue. We explored the effects of the number of bridging C bases between G and T on the efficiencies of intrastrand cross-link formation in the series of oligonucleotides 5′-d(GpC_npT) and 5′-d(TpC_npG) with $n = 0$, 1, 2 and 3. The intrastrand cross-links generated by the oxidation of these sequences by $CO_3^{\bullet-}$ radicals were isolated by HPLC and identified by LC-MS/MS methods. The positive ion spectra of the cross-linked product, 5′-d(G*pT*) derived from the oxidation of the dinucleotide, 5′-d(GpT) exhibits a molecular ion, $[M + H]^+$ at m/z 570.3, as well as the characteristic ion at m/z 276.2 arising from the fragmentation of $[M + H]^+$ (Figure S2, Supplementary Data). The cross-linked product, 5′-d(G*CCT*) generated by the oxidation of 5′-d(GCCT) was identified using the negative ion spectrum that shows molecular ions, $[M - H]^-$ at m/z 1146.4 and $[M - 2H]^{2-}$ at m/z 572.9 (Figure S3, Supplementary Data).

The highest efficiency of intrastrand 5′-d(G*pCpT*) cross-link formation is found in the 5′-d(GpCpT) sequence; in the case of 5′-d(GpT) without intervening C

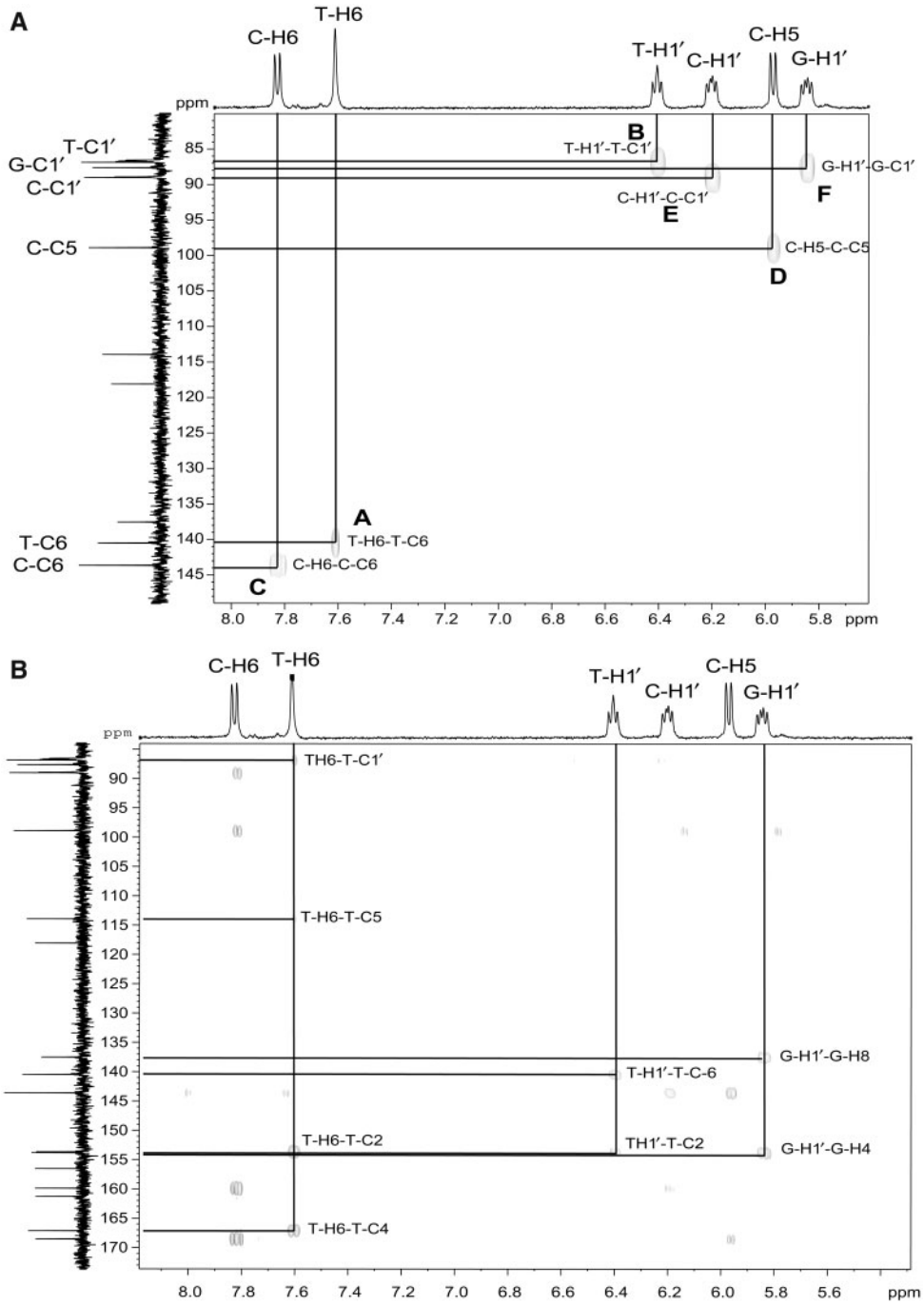

Figure 8. (**A**) Portion of the 2-D HSQC NMR spectrum of 5′-d(G*pCpT*) showing the correlations that allow assignment of C-C5, C-C6, T-C6 and the C1′ carbons of each guanine, cytosine and thymine residue. (**B**) Portion of the 2-D HMBC NMR spectrum of 5′-d(G*pCpT*) showing some of the multiple bond correlations that allow assignment of the aromatic base carbons with no attached protons.

bases the efficiency is almost three times lower (Figure 9). Increasing the number of the C bases also resulted in a decrease in the efficiency of cross-link formation when there are two C bridging residues as in the case of 5′-d(GCCT). In the case of 5′-d(GCCCT), sequence with three bridging C residues the cross-linked products were not detected. Furthermore, the intrastrand 5′-d(T*pG*) cross-links were not detected in 5′-d(TpG), although there is a substantial yield in the isomeric 5′-d(GpT) (Figure 6). This latter result supports the conclusion, reached on the basis of experiments with the isomeric 5′-d(GpCpT) and 5′-d(TpCpG), that the cross-link formation is more efficient when the T residue is on the 3′-side rather than on the 5′-side of the guanine.

Cross-link formation in DNA duplexes

The formation of cross-links between *adjacent* G and T bases in oligonucleotides by ionizing radiation has

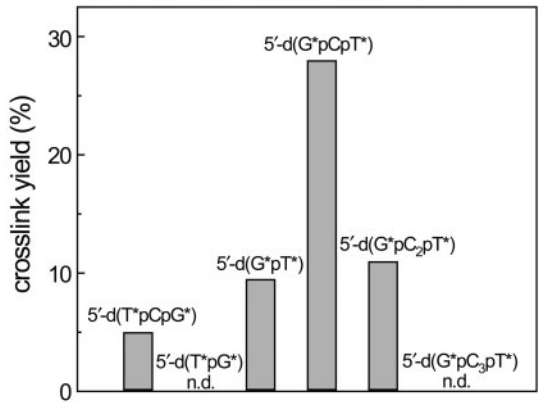

Figure 9. Yields of intrastrand cross-linked lesions derived from of 5′-d(GpC$_n$pT) and 5′-d(TpC$_n$pG) sequences (0.01 mM) by $CO_3^{\bullet-}$ radicals. The reaction conditions were identical to those used for generating the results shown in Figure 2.

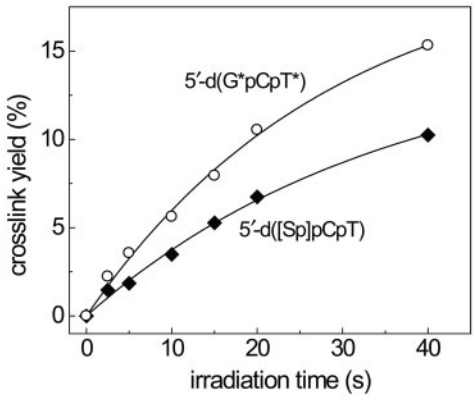

Figure 10. Time-dependent yields of the 5′-d(G*pCpT*) and 5′-d([Sp]pCpT) products generated by $CO_3^{\bullet-}$ radicals. The reaction conditions were identical to those used for generating the results shown in Figure 2. The yields were calculated from the integrated peak areas in the HPLC elution profiles and the molecular absorptivities at 260 nm of 5′-d(GpCpT) ($3 \times 10^3\ M^{-1}cm^{-1}$), 5′-d(G*pCpT*) ($3 \times 10^3\ M^{-1}cm^{-1}$) and 5′-d([Sp]pCpT) ($3 \times 10^3\ M^{-1}cm^{-1}$).

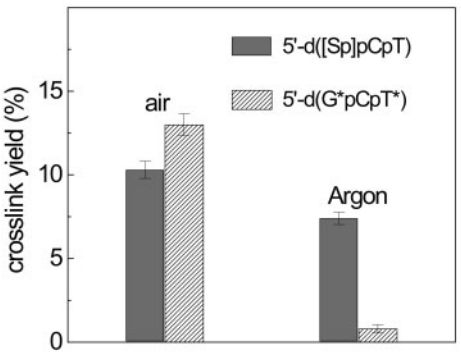

Figure 11. Yields of the 5′-d(G*pCpT*) and 5′-d([Sp]pCpT) products generated by $CO_3^{\bullet-}$ radicals. The reaction conditions were identical to those used for generating the results shown in Figure 2. The yields were calculated from the integrated peak areas in the HPLC elution profiles and the molecular absorptivities at 260 nm.

been extensively studied by Box *et al.* (15–19), Cadet *et al.* (20–22) and by Hong *et al.* (23,24). Here, we investigated whether oxidation of oligonucleotides by $CO_3^{\bullet-}$ radicals can also induce cross-linking reactions in double-stranded DNA and whether the linkage formed involves the T5-CH_3 methyl as in the experiments initiated by ionizing radiation. To test this hypothesis, we explored the oxidation of the duplex derived from the self-association of the self-complementary sequence, 5′-d(TTACG TACGTAA) with adjacent G and T nucleotides by $CO_3^{\bullet-}$ radicals. After the reactions, the oxidized duplexes were desalted, enzymatically digested by nuclease P1 and alkaline phosphatase, and the products were separated by reversed-phase HPLC methods. The digestion product eluting at 4.1 min after dC at 3.1 min (Figure S8A in Supplementary Data), was desalted, concentrated and subjected to LC-MS/MS analysis. The positive ion spectra (MS/MS) of this digestion product (Figure S8B, Supplementary Data) are identical to the spectra of a 5′-d(G*pT*) cross-link standard (Figure S2) prepared by the oxidation of the dinucleotide 5′-d(GpT) by $CO_3^{\bullet-}$ radicals. We also found that the 5′-d(G*pT*) sequence excised from the self-complementary duplex exposed to $CO_3^{\bullet-}$ radicals co-elutes with the 5′-d(G*pT*) standard and that the phosphate group between G and T bases is thus not removed by the treatment of 5′-d(G*pT*) with nuclease P1 and alkaline phosphatase. In contrast, such a treatment in the case of the 5′-d(G*pCpT*) sequence removes the pCp moiety thus leaving a residual G*-T* cross-linked product (Figures 2 and 3). The yields of the G*pT* cross-links in the double-stranded DNA are lower than in the case of 5′-d(GpT) dinucleosides and do not exceed 2–3%.

Role of different one-electron oxidants in the cross-linking reaction

Our experiments have shown that the highest yields of the G*-T* cross-links are observed in the case of 5′-d(GpCpT). Using this trinucleotide we found that the yields of the two major products, 5′-d(G*pCpT*) and 5′-d([Sp]pCpT) increase monotonically with increasing irradiation time as shown in Figure 10. These observations can be considered as an indication that 5′-d(G*pCpT*) and 5′-d([Sp]pCpT) are formed via two parallel processes and that the cross-linked product 5′-d(G*pCpT*) is generated by a two-electron oxidation of 5′-d(GpCpT) and is not a precursor of the 5′-d([Sp]pCpT) product derived from a four-electron oxidation of guanine in 5′-d(GpCpT). Removal of O_2 by purging the sample solutions with argon during the irradiation significantly decreases the yield of the cross-linked 5′-d(G*pCpT*) product by a factor of 16; in contrast, the yield of 5′-d([Sp]pCpT) decreases by factor of only 1.4 (Figure 11). Since, the cross-linked product does not contain any additional oxygen atoms in comparison with the parent 5′-d(GpCpT), we propose that oxygen is required for the oxidation of the intermediates. In agreement with our previous ^{18}O-isotope labeling experiments, which have shown that the major

Table 3. Yields (%) of trinucleotide oxidation products from 5′-d(GpCpT) generated by one-electron oxidants in air-equilibrated buffer solutions (pH 7.5) containing 20 mM $Na_2S_2O_8$ or 15 μM RF

Oxidant	E°, V versus NHE	5′-d(G*pCpT*)	5′-d([Sp]pCpT)	5′-d([Iz]pCpT)[a]
$SO_4^{\bullet-}$	2.43 (39)	5.6	n.d.[b]	4.0
[c]$CO_3^{\bullet-}$	1.59 (39)	13.0	10.3	2.3
[d]$N_3^{\bullet}$	1.33 (40)	n.d.[b]	n.d.	n.d.
*Riboflavin[e]	~1.7[f] (42)	6.0	3.1	11.5

[a]Identified by the characteristic molecular ion, $[M + H - 39]^+$ at m/z 822.2 (43).
[b]Not detected.
[c]$[HCO_3^-] = 0.3$ M.
[d]$[N_3^-] = 0.1$ M.
[e]Electronically excited riboflavin; [f]For $^3RF/RF^{\bullet-}$.

pathway of 5′-d([Sp]pCpT) formation involves a consecutive four-electron oxidation of 5′-d(GCT) mediated by carbonate radicals (12), oxygen is not critical for the formation of the Sp lesions.

Further experiments performed in air-equilibrated solutions have shown that carbonate radicals are not uniquely necessary for the generation of the cross-linked 5′-d(G*pCpT*) products. To explore these issues further, we used a series of one-electron oxidants with different reduction potentials (39,40) as well as riboflavin (RF), a typical type I photosensitizer that reacts with DNA via electron abstraction mechanisms (41), to oxidize the trinucleotide 5′-d(GpCpT). The results are summarized in Table 3. After irradiation (30 s, ~100 mW/cm^2), the end products were separated by reversed-phase HPLC methods and analyzed by LC-MS/MS that allowed us to identify three major end products: 5′-d(G*pCpT*), 5′-d([Sp]pCpT) and 5′-d([Iz]pCpT), where Iz is 2,5-diamino-4H-imidazolone. The results of these experiments summarized in Table 3 show that the generation of the end products from 5′-d(GpCpT) correlate with the reduction potential of the oxidant.

The reduction potential of carbonate radical of 1.59 V versus NHE (39) is greater than that of guanine neutral radical, 1.29 V versus NHE (9) and the 5′-d(G*pCpT*) and 5′-d([Sp]pCpT) are the major end products, but minor quantities of 5′-d([Iz]pCpT) are also observed. The $SO_4^{\bullet-}$ radical, a stronger one-electron oxidant with the reduction potential of 2.43 V versus NHE (39), oxidizes 5′-d(GpCpT) thus forming 5′-d(G*pCpT*) and 5′-d([Iz]pCpT) as the major oxidation products, but 5′-d([Sp]pCpT) products are not generated. The azide radical, which is a mild one-electron oxidant with a reduction potential of 1.33 V versus NHE (40), was generated by the oxidation of the azide anion by photochemically generated $SO_4^{\bullet-}$ radicals. In order to minimize the reactions with nucleotides, the $SO_4^{\bullet-}$ radicals were trapped by high concentrations of N_3^- anions (0.1 M). Under these conditions, the $N_3^{\bullet}$ radicals do not produce well-defined products such as 5″-d(G*pCpT*), 5′-d([Sp]pCpT) and 5′-d([Iz]pCpT). The value of $E^\circ = 1.33$ V versus NHE for $N_3^{\bullet}$ radicals is very close to that of 1.29 V versus NHE for dG(-H)$^{\bullet}$ (9), and under our experimental conditions ($[N_3^-] = 0.1\ M \gg [d(GpCpT)] = 0.1$ mM, Table 1) the driving force of one-electron oxidation of guanine by $N_3^{\bullet}$ radicals is not sufficient for the generation of oxidation products of 5′-d(GpCpT) with observable rates. In contrast, utilizing RF as the photosensitizer which, in the triplet excited state, has a reduction potential of ~1.7V versus NHE (42), all three products, 5′-d(G*pCpT*), 5′-d([Sp]pCpT) and 5′-d([Iz]pCpT) are generated, with d([Iz]pCpT) being the major product (Table 3). In the case of free nucleosides, photosensitization of the oxidation of dG by RF generates dIz, dSp and cdG [2,5′-anhydro-l-(2′-deoxy-β-D-*erythro*-pentofuranosyl)-5-guanidinylidene-2-hydroxy-4-oxoimidazolidine] cyclonucleoside products (41).

DISCUSSION

Structural characterization of the 5′-d(G*pCpT*) lesion

The 1D proton NMR data clearly indicate that the G-C8 proton is missing in the cross-linked product, thus suggesting that guanine is covalently linked to T via its C8 carbon atom. The T-CH_3 methyl group protons are characterized by the usual single resonance at 1.85 p.p.m. (Table 1), indicating that all three protons are present and the covalent linkage to guanine does not involve the thymine methyl group. The ^{13}C chemical shift at 14.28 p.p.m. (Table 2) is consistent with an sp^3 hybridization of the methyl group carbon atom, and is in agreement with the conclusions derived from the 1D NMR spectrum. The T-H6 proton resonates at 7.61 p.p.m. in the ^1H spectrum, and the HSQC correlation diagram (Figure 8A) identifies the T-C6 ^{13}C resonance at 140.49 p.p.m.; the T-C1′ resonance can also be identified via its cross-peak in the HMBC spectrum (Figure 8B). The downfield ^{13}C chemical shift of T-C6 in the 5′-d(G*pCpT*) product is close to the 139.73 p.p.m. value for T-C6 in the 5′-d(CpGpT) control indicating that sp^2 hybridization is intact (Figure S4B and S4D in Supplementary Data). Similarly, the chemical shifts of the T-C5 carbon atom at 113.90 p.p.m. in 5′-d(G*pCpT*) and 113.85 p.p.m. in the 5′-d(GpCpT) control, indicate that the T-C5/T-C6 double bond is intact. These observations demonstrate that neither T-C5 nor T-C6 are involved in the covalent bond formation between G-C8 and thymidine in the 5′-d(G*pCpT*) product. The T-C2 and T-C4 ^{13}C resonances at 153.69 and 167.16 p.p.m., respectively, are close to the analogous values at 151.91 and 168.65 p.p.m. in the 5′-d(GpCpT) control; these downfield chemical shifts are consistent with carbon atoms in carbonyl groups and suggest that the covalent linkage between G-C8 and thymine does not involve the T-C2 or T-C4 carbonyl oxygen atoms. Thus, none of the chemical shifts in the carbon atoms in thymidine appear to be significantly different in the cross-linked product and the control 5′-d(GpCpT) sequence. This is in agreement with ^{13}C NMR data for 3-methyl thymidine, where *N*-functionalization results in minimal changes in the chemical shifts of the other carbon atoms in the modified base (44).

The G-H1′ multiplet at 5.82–5.86 p.p.m. (see, Supplementary Data for the assignment) shows HMBC correlations to two ^{13}C signals at 137.5 p.p.m. and 153.8 p.p.m. (Figure 8B), which can be expected to represent G-C4 and G-C8. Literature values for the G-C4 and G-C8 resonances (44) suggest that G-C4 is the signal at 153.8 p.p.m. and G-C8 is the signal at 137.5 p.p.m. The ^{13}C signal of the G-C8 atom in guanine derivatives functionalized in the C8-position might be expected to undergo a downfield shift relative to the unmodified nucleoside, at least based on the substitution of H by N at the G-C8 position. However, the chemical shift of this G-C8 resonance has not changed significantly in 5′-(G*pCpT*) (137.50 p.p.m.) relative to the unmodified 5′-d(GpCpT) (140.13 p.p.m.) (Figure S4B and S4D in Supplementary Data). As in our case, no significant downfield shifts have been observed in the case of *N*-(2′-deoxyguanosin-8-yl)-2,4-dimethylaniline where G-C8 resonates at 138.0 p.p.m. (45), although a downfield shift from 136.2 to 143.2 p.p.m. was reported in the case of 8-(*N*-fluoren-2-ylacetamido)-2′-deoxyguanosine 5′-monophosphate (46).

Overall, an analysis of the ^{13}C NMR spectra suggests that the covalent link between G and T in the 5′-d(G*pCpT*) product occurs via the G-C8 and T-N3 atoms. The G-C8/T-N3 bond may account for the pronounced shift of the H1′ and H2′/H2″ protons because the constrained relative orientations of the G-T bases may influence the syn/anti configuration of the ribose units thus affecting the magnetic environment of these H1′, H2′, H2″ protons. However, more extensive studies that were beyond the scope of this work would be needed to confirm this hypothesis.

The conclusions based on the NMR data are supported by the experiments involving acid hydrolysis of the cross-linked 5′-d(G*pCpT*) sequence, followed by LC-MS/MS analysis (Figure 6) that clearly indicates formation of a G*-dT* hydrolysis product. Fragmentation of the corresponding molecular ion, $[M + H]^+$ at *m*/*z* 392.0] ion leads to the loss of the sugar residue to yield the base-base heterodimer product G*-T* (*m*/*z* 276.0). Further cleavage of the N3–C4 and C2–N1 bonds of thymine yields the ions *m*/*z* 192.9 and *m*/*z* 84.2 (Figure 6). These patterns are typical of the fragmentation of thymine derivatives (37) and suggest that only the N3 or O2 atoms of thymine can be covalently linked to guanine in the G*-T* cross-linked product. Since any C8–O2 (or C8–O4) bonds should be unstable under conditions of acid hydrolysis, we conclude that the cross-link in the G*-T8 product occurs via a G-C8/T-N3 bond rather than a G-C8/T-O linkage, in agreement with the NMR results.

Comparison with other oxidatively generated DNA cross-linked products

The pioneering work of Box and co-workers (15–19) has provided experimental evidence that ionizing radiation produces intrastrand cross-links between the adjacent G and T bases, thus generating the so-called tandem lesions in deoxygenated solutions. A similar G*pT* intrastrand cross-link was also observed when native DNA was subjected to oxidation by a Fenton reaction pathway (24). In these tandem lesions, the C8-atom of guanine is bound to the C-atom of the methyl group in thymine and the formation of these lesions involves intermediate formation of the C-centered 5-(2′-deoxyuridinyl)methyl radicals. Cadet and co-workers (20–22) have reported that molecular oxygen completely suppresses the formation of such tandem lesions, probably due to the fast reaction of 5-(2′-deoxyuridinyl)methyl radicals with oxygen, and that tandem lesions formed in the presence of O_2 are composed from the oxygenated G and T bases in DNA. In contrast, Greenberg and co-workers (14,47,48) have proposed that reaction of 5-(2′-deoxyuridinyl)methyl radicals with O_2 is reversible [$k(O_2) = 2 \times 10^9\ M^{-1}s^{-1}$, and $k_{-}(O_2) = 3.4\ s^{-1}$] and that molecular oxygen does not prevent the addition of these radicals to adenine. Our experiments demonstrate that oxidation of the single-stranded oligonucleotides by $CO_3^{\bullet-}$ radicals generate a new type of intrastrand cross-link between G and T bases separated by 0, 1 and 2 cytosine bases and the presence of oxygen is required for formation of these cross-links (Figure 11). High-resolution NMR studies show that in these lesions the H-atom at the C6 of thymine, the CH_3-group of thymine and the H-atoms at the C5 and C6 positions of cytosine remain intact. These observations, coupled to the loss of 2 Da in the cross-linked products are consistent with a covalent bond formation between the C8-atom of guanine and the N3 atom of thymine (Figure 1). These new lesions do not require the formation of 5-(2′-deoxyuridinyl)methyl radicals that typically react rapidly with molecular oxygen (48) and $CO_3^{\bullet-}$ radicals generate these cross-links in air-equilibrated solutions.

Mechanistic considerations

The cross-linking reaction in the GCT sequence is triggered by the one-electron abstraction from guanine bases by $CO_3^{\bullet-}$ radicals (Figure 12). This step can be initiated by other one-electron oxidants with appropriate reduction potentials (Table 3). The guanine neutral radicals, G(-H)$^\bullet$ generated by $CO_3^{\bullet-}$ radicals in single- and double-stranded DNA were detected by a direct spectroscopic approach in our previous experiments (10,11,49). The G(-H)$^\bullet$ radicals do not react with observable rates with oxygen (10,11) and their fates are determined by further reactions with free radicals or nucleophiles (2,50). Perrier *et al.* (51) have shown that the RF-mediated photosensitization of d(TpGpT) in aerated solutions containing the KKK tripeptide gives rise to an efficient cross-linking reaction between the guanine and lysine residues. These authors suggested that the cross-linking reaction occurs via a nucleophilic addition of the ε-amino group of the lysine residue to the C8 atom of the $G^{\bullet+}$ or G(-H)$^\bullet$ radicals followed by oxidation of the radical adduct formed to the *N*ε-(guanin-8-yl)-lysine cross-link. Here, we propose a similar mechanism for the formation of the G*-T* cross-link that includes the nucleophilic addition of the N3 atom of the thymine residue to the C8 atom of the guanine radical (Figure 12). The radical adduct formed can be oxidized by O_2 to abstract the second electron that is required for the

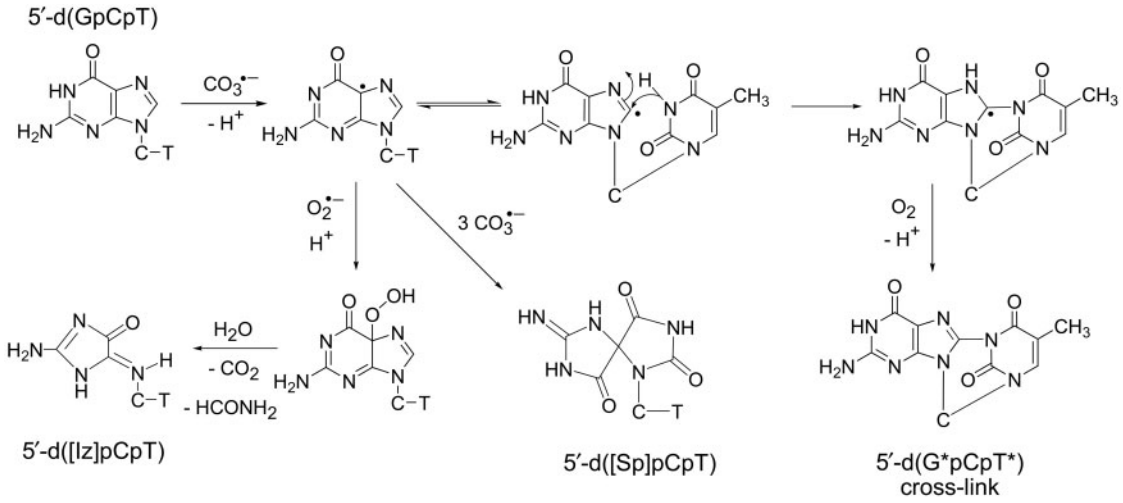

Figure 12. Mechanism of 5′-d(GpCpT) oxidation by carbonate radical anions.

cross-linking reaction. An alternative mechanism might involve the oxidation of the thymidine base ('second hit'), followed by the combination reaction of the guanine and thymine radicals. Since $CO_3^{\bullet-}$ radicals are not capable of oxidizing thymine bases with observable rates (10), only the $SO_4^{\bullet-}$ radicals can oxidize T in our experiments. However, this mechanism seems unlikely since ESR studies have shown that the yields of N3-centered thymine radicals generated by $SO_4^{\bullet-}$ radicals are negligible (52). Isolation and structural analysis of T-T dimer formation produced by ionizing radiation and subsequent radical–radical interactions provides further evidence that the yields of N3-centered T radicals are small in comparison to the yields of radicals centered at T-CH3, C5 and C6 (53). Therefore, it is unlikely that a bimolecular radical-radical reaction mechanism could have produced G-C8/T-N3 cross-links as efficiently as observed here in the 5′-d(GpCpT) sequences (Figure 9 and Table 3).

Once the oxidation of guanines by the carbonate radicals produce the G(-H)$^\bullet$ radicals, the latter can react either by the nucleophilic addition of N3 of thymine to G-C8 thus forming the crosslinked product, or by competitive reactions with other radicals such as CO3$^{\bullet-}$ and O2$^{\bullet-}$ to form the Sp and Iz products instead (Figure 12). Our laser transient absorbance photolysis experiments have shown that the rate constants of oxidation of G by $CO_3^{\bullet-}$ radicals depends weakly on the secondary DNA structure and sequence context [rate constants in the range of $(2–7) \times 10^7\,M^{-1}s^{-1}$] and are typically smaller by 1–2 orders of magnitude than the rate constants of the subsequent bimolecular reactions with radical and non-radical intermediates (10,11,49). Indeed, ^{18}O-isotope analysis of the end products of the guanine oxidation by $CO_3^{\bullet-}$ radicals has shown that the G(-H)$^\bullet$, 8-oxo-dG and 8-oxo-dG(-H)$^\bullet$ intermediates efficiently react with $CO_3^{\bullet-}$ radicals and that the Sp diastereomers formed contain two oxygen atoms derived from $CO_3^{\bullet-}$ radicals (12). In contrast, reactions of $SO_4^{\bullet-}$ radicals with guanines are extremely fast and the rate constants are close to diffusion-controlled ($4.3 \times 10^9\,M^{-1}s^{-1}$ for dG) (54). The subsequent consecutive three-electron oxidation of the G(-H)$^\bullet$ radicals by the $SO_4^{\bullet-}$ radicals that could result in the formation of the Sp diastereomers (10–12), cannot compete with the reactions of $SO_4^{\bullet-}$ radicals with G that is in excess of G(-H)$^\bullet$ under our experimental conditions and, therefore such end products are not observable (Table 3).

The formation of the Iz lesions is associated with the combination of G(-H)$^\bullet$ radicals and superoxide radicals (2,26,50). This reaction dominates in the case of the RF-mediated photosensitization of 5′-d(GCT) in air-equilibrated solutions (Table 3). Although, the mechanism of the RF-mediated photosensitization of guanines in DNA remains unknown (41), we propose that the triplet excited state of RF can initiate oxidation reactions. Indeed, 2′-deoxyguanosine 5′-monophosphate is rapidly oxidized by the triplet excited state of RF ($6.6 \times 10^8\,M^{-1}s^{-1}$) to produce the G(-H)$^\bullet$ and RF-semiquinone radicals (55). The latter radicals efficiently generate $O_2^{\bullet-}$ radicals in the reaction with oxygen (42). The efficient formation of the Iz lesions mediated by RF photosensitization has been detected in free nucleosides (56) and in single- and double-stranded DNA (57). The formation of $O_2^{\bullet-}$ radicals can also be triggered by the oxidation of 5′-d(GpCpT) by $SO_4^{\bullet-}$ radicals. The $SO_4^{\bullet-}$ radicals can oxidize all three bases in 5′-d(GpCpT) because these radicals rapidly react with dG [$4.3 \times 10^9\,M^{-1}s^{-1}$ (54)], dT [$2.1 \times 10^9\,M^{-1}s^{-1}$ (58)] and dC [$1.6 \times 10^9\,M^{-1}s^{-1}$ (59)] to mostly form radicals of the nucleobases. The G(-H)$^\bullet$ radicals are oxidizing and do not react with oxygen (10,11). In contrast, the oxidation of the pyrimidine bases generates C-centered radicals that rapidly react with oxygen to form peroxyl radicals (58,59). Experiments performed in our laboratory have shown that the combination of G(-H)$^\bullet$ and peroxyl radicals can result in the formation of Iz lesions.

Biological implications

The intrastrand crosslinking reaction reported here that covalently couples G and T in the 5′-….GC_nT…3′ sequence context is triggered by the carbonate radical

anion. The $CO_3^{\bullet-}$ radical is a ubiquitous byproduct of the inflammatory response (1,2) and can easily oxidize guanine in single- and double-stranded DNA by a one-electron transfer mechanism (10–12,49). In the absence of other radicals and further oxidative reactions, neutral guanine radical, G(-H)$^\bullet$ derived from the deprotonation of the guanine radical cation, G(-H)$^{\bullet+}$, has a lifetime that approaches seconds (10,11), and reaction of G(-H)$^\bullet$ with T can occur by the nucleophilic N3 addition mechanism described (Figure 12). Oxygen is abundant and can oxidize the G-T radical adduct thus forming the superoxide anion in the process. This O_2-mediated reaction thus should add to the oxidative stress associated with $CO_3^{\bullet-}$ radicals. The formation of G*-T* crosslinks requires a single hit by a one-electron oxidant, and is of course sequence dependent. The reparability of these novel cross-linked lesions by different DNA repair systems is not yet known, but is under study in our laboratory.

SUPPLEMENTARY DATA

Supplementary Data are available at NAR online.

ACKNOWLEDGEMENTS

We thank Dr C. H. Lin for insightful discussion of the NMR experiments. This work was supported by the National Institute of Environmental Health and Sciences (5 R01 ES 011589-06), and by the Kresge Foundation. Components of this work were conducted in the Shared Instrumentation Facility at NYU that was constructed with support from Research Facilities Improvement (C06 RR-16572) from the National Center for Research Resources, National Institutes of Health. The acquisition of the 500MHz spectrometer and ion trap were supported by the National Science Foundation (MRI 0116222 and CHE-0234863, respectively). Funding to pay the Open Access publication charge was provided by the National Institute of Environmental Health and Sciences (5 R01 ES 011589-06).

Conflict of interest statement. None declared.

REFERENCES

1. Dedon,P.C. and Tannenbaum,S.R. (2004) Reactive nitrogen species in the chemical biology of inflammation. *Arch. Biochem. Biophys.*, **423**, 12–22.
2. Cadet,J., Douki,T. and Ravanat,J.L. (2006) One-electron oxidation of DNA and inflammation processes. *Nat. Chem. Biol.*, **2**, 348–349.
3. Beckman,J.S., Beckman,T.W., Chen,J., Marshall,P.A. and Freeman,B.A. (1990) Apparent hydroxyl radical production by peroxynitrite: implications for endothelial injury from nitric oxide and superoxide. *Proc. Natl Acad. Sci. USA*, **87**, 1620–1624.
4. Davis,K.L., Martin,E., Turko,I.V. and Murad,F. (2001) Novel effects of nitric oxide. *Annu. Rev. Pharmacol. Toxicol.*, **41**, 203–236.
5. Ischiropoulos,H. and Beckman,J.S. (2003) Oxidative stress and nitration in neurodegeneration: cause, effect, or association? *J. Clin. Invest.*, **111**, 163–169.
6. Pacher,P., Beckman,J.S. and Liaudet,L. (2007) Nitric oxide and peroxynitrite in health and disease. *Physiol. Rev.*, **87**, 315–424.
7. Lymar,S.V. and Hurst,J.K. (1995) Rapid reaction between peroxonitrite ion and carbon dioxide: implications for biological activity. *J. Am. Chem. Soc.*, **117**, 8867–8868.
8. Goldstein,S. and Czapski,G. (1999) Viscosity effects on the reaction of peroxynitrite with CO_2: Evidence for radical formation in a solvent cage. *J. Am. Chem. Soc.*, **121**, 2444–2447.
9. Steenken,S. and Jovanovic,S.V. (1997) How easily oxidizable is DNA? One-electron reduction potentials of adenosine and guanosine radicals in aqueous solution. *J. Am. Chem. Soc.*, **119**, 617–618.
10. Shafirovich,V., Dourandin,A., Huang,W. and Geacintov,N.E. (2001) Carbonate radical is a site-selective oxidizing agent of guanines in double-stranded oligonucleotides. *J. Biol. Chem.*, **276**, 24621–24626.
11. Joffe,A., Geacintov,N.E. and Shafirovich,V. (2003) DNA lesions derived from the site-selective oxidation of guanine by carbonate radical anions. *Chem. Res. Toxicol.*, **16**, 1528–1538.
12. Crean,C., Geacintov,N.E. and Shafirovich,V. (2005) Oxidation of guanine and 8-oxo-7,8-dihydroguanine by carbonate radical anions: insight from oxygen-18 labeling experiments. *Angew. Chem. Int. Ed. Engl.*, **44**, 5057–5060.
13. Box,H.C., Dawidzik,J.B. and Budzinski,E.E. (2001) Free radical-induced double lesions in DNA. *Free Radic. Biol. Med.*, **31**, 856–868.
14. Greenberg,M.M. (2007) Elucidating DNA damage and repair processes by independently generating reactive and metastable intermediates. *Org. Biomol. Chem.*, **5**, 18–30.
15. Box,H.C., Budzinski,E.E., Dawidzik,J.D., Wallace,J.C., Evans,M.S. and Gobey,J.S. (1996) Radiation-induced formation of a crosslink between base moieties of deoxyguanosine and thymidine in deoxygenated solutions of d(CpGpTpA). *Radiat. Res.*, **145**, 641–643.
16. Box,H.C., Budzinski,E.E., Dawidzik,J.B., Gobey,J.S. and Freund,H.G. (1997) Free radical-induced tandem base damage in DNA oligomers. *Free Radic. Biol. Med.*, **23**, 1021–1030.
17. Budzinski,E.E., Dawidzik,J.B., Rajecki,M.J., Wallace,J.C., Schroder,E.A. and Box,H.C. (1997) Isolation and characterization of the products of anoxic irradiation of d(CpGpTpA). *Int. J. Radiat. Biol.*, **71**, 327–336.
18. Box,H.C., Budzinski,E.E., Dawidzik,J.B., Wallace,J.C. and Iijima,H. (1998) Tandem lesions and other products in X-irradiated DNA oligomers. *Radiat. Res.*, **149**, 433–439.
19. Box,H.C., Budzinski,E.E., Dawidzik,J., Patrzyc,H.B. and Freund,H.C. (2001) A novel double lesion in X-irradiated DNA consists of a strand break and a base modification. *Radiat. Res.*, **156**, 215–219.
20. Delatour,T., Douki,T., Gasparutto,D., Brochier,M.C. and Cadet,J. (1998) A novel vicinal lesion obtained from the oxidative photosensitization of TpdG: characterization and mechanistic aspects. *Chem. Res. Toxicol.*, **11**, 1005–1013.
21. Romieu,A., Bellon,S., Gasparutto,D. and Cadet,J. (2000) Synthesis and UV photolysis of oligodeoxynucleotides that contain 5-(phenylthiomethyl)-2′-deoxyuridine: a specific photolabile precursor of 5-(2′-deoxyuridilyl)methyl radical. *Org. Lett.*, **2**, 1085–1088.
22. Douki,T., Riviere,J. and Cadet,J. (2002) DNA tandem lesions containing 8-oxo-7,8-dihydroguanine and formamido residues arise from intramolecular addition of thymine peroxyl radical to guanine. *Chem. Res. Toxicol.*, **15**, 445–454.
23. Zhang,Q. and Wang,Y. (2004) Independent generation of the 5-hydroxy-5,6-dihydrothymidin-6-yl radical and its reactivity in dinucleoside monophosphates. *J. Am. Chem. Soc.*, **126**, 13287–13297.
24. Hong,H., Cao,H., Wang,Y. and Wang,Y. (2006) Identification and quantification of a guanine-thymine intrastrand cross-link lesion unduced by Cu(II)/H_2O_2/ascorbate. *Chem. Res. Toxicol.*, **19**, 614–621.
25. Kornyushyna,O., Berges,A.M., Muller,J.G. and Burrows,C.J. (2002) In vitro nucleotide misinsertion opposite the oxidized guanosine lesions spiroiminodihydantoin and guanidinohydantoin and DNA synthesis past the lesions using *Escherichia coli* DNA polymerase I (Klenow fragment). *Biochemistry*, **41**, 15304–15314.
26. Misiaszek,R., Uvaydov,Y., Crean,C., Geacintov,N.E. and Shafirovich,V. (2005) Combination reactions of superoxide with 8-oxo-7,8-dihydroguanine radicals in DNA: Kinetics and end-products. *J. Biol. Chem.*, **280**, 6293–6300.
27. Ravanat,J.L. and Cadet,J. (1995) Reaction of singlet oxygen with 2′-deoxyguanosine and DNA. Isolation and characterization of the main oxidation products. *Chem. Res. Toxicol.*, **8**, 379–388.

28. Durandin,A., Jia,L., Crean,C., Kolbanovskiy,A., Ding,S., Shafirovich,V., Broyde,S. and Geacintov,N.E. (2006) Assignment of absolute configurations of the enantiomeric spiroiminodihydantoin nucleobases by experimental and computational optical rotatory dispersion methods. *Chem. Res. Toxicol.*, **19**, 908–913.
29. Sannes-Lowery,K.A., Mack,D.P., Hu,P., Mei,H.-Y. and Loo,J.A. (1997) Positive ion electrospray ionization mass spectrometry of oligonucleotides. *J. Am. Soc. Mass Spectrom.*, **8**, 90–95.
30. Ni,J., Mathews,M.A.A. and McCloskey,J.A. (1997) Collision-induced dissociation of polyprotonated oligonucleotides produced by electrospray ionization. *Rapid Commun. Mass Spectrom.*, **11**, 535–540.
31. Wang,P.P., Bartlett,M.G. and Martin,L.B. (1997) Electrospray collision-induced dissociation mass spectra of positively charged oligonucleotides. *Rapid Commun. Mass Spectrom.*, **11**, 846–856.
32. Burrows,C.J. and Muller,J.G. (1998) Oxidative nucleobase modifications leading to strand scission. *Chem. Rev.*, **98**, 1109–1151.
33. Douki,T., Delatour,T., Paganon,F. and Cadet,J. (1996) Measurement of oxidative damage at pyrimidine bases in γ-irradiated DNA. *Chem. Res. Toxicol.*, **9**, 1145–1151.
34. Garrett,E.R., Seydel,J.K. and Sharpen,A.J. (1966) The acid-catalyzed solvolysis of pyrimidine nucleosides. *J. Org. Chem.*, **31**, 2219–2227.
35. Hevesi,L., Wolfson-Davidson,E., Nagy,J.B., Nagy,O.B. and Bruylants,A. (1972) Contribution to the mechanism of the acid-catalyzed hydrolysis of purine nucleosides. *J. Am. Chem. Soc.*, **94**, 4715–4720.
36. Cadet,J. and Teoule,R. (1974) Nucleic acid hydrolysis. I. Isomerization and anomerization of pyrimidic deoxyribonucleosides in an acidic medium. *J. Am. Chem. Soc.*, **96**, 6517–6519.
37. Rice,J.M., Dudek,G.O. and Barber,M. (1965) Mass spectra of nucleic acid derivatives. Pyrimidines. *J. Am. Chem. Soc.*, **87**, 4569–4576.
38. Singer,B., Kroger,M. and Carrano,M. (1978) O2- and O4-alkyl pyrimidine nucleosides: stability of the glycosyl bond and of the alkyl group as a function of pH. *Biochemistry*, **17**, 1246–1250.
39. Huie,R.E., Clifton,C.L. and Neta,P. (1991) Electron transfer reaction rates and equilibria of the carbonate and sulfate radical anions. *Radiat. Phys. Chem.*, **38**, 477–481.
40. Stanbury,D.M. (1989) Reduction potentials involving inorganic free radicals in aqueous solution. *Adv. Inorg. Chem.*, **33**, 69–138.
41. Ravanat,J.L., Saint-Pierre,C. and Cadet,J. (2003) One-electron oxidation of the guanine moiety of 2′-deoxyguanosine: Influence of 8-oxo-7,8-dihydro-2′-deoxyguanosine. *J. Am. Chem. Soc.*, **125**, 2030–2031.
42. Yoshimura,A. and Ohno,T. (1988) Lumiflavin-sensitized photooxygenation of indole. *Photochem. Photobiol.*, **48**, 561–565.
43. Gasparutto,D., Ravanat,J.-L., Gerot,O. and Cadet,J. (1998) Characterization and chemical stability of photooxidized oligonucleotides that contain 2,2-diamino-4-[(2-deoxy-β-D-erythro-pentofuranosyl)amino]-5(2*H*)-oxazolone. *J. Am. Chem. Soc.*, **120**, 10283–10286.
44. Chang,C.-J., DaSilva Gomes,J. and Byrn,S.R. (1983) Chemical modification of deoxyribonucleic acids: a direct study by carbon-13 nuclear magnetic resonance spectroscopy. *J. Org. Chem.*, **48**, 5151–5160.
45. Marques,M.M., Mourato,L.L., Santos,M.A. and Beland,F.A. (1996) Synthesis, characterization, and conformational analysis of DNA adducts from methylated anilines present in tobacco smoke. *Chem. Res. Toxicol.*, **9**, 99–108.
46. Evans,F.E., Miller,D.W. and Levine,R.A. (1984) Conformation and dynamics of the 8-substituted deoxyguanosine 5′-monophosphate adduct of the carcinogen 2-(acetylamino)fluorene. *J. Am. Chem. Soc.*, **106**, 396–401.
47. Hong,I.S. and Greenberg,M.M. (2005) Efficient DNA interstrand cross-link formation from a nucleotide radical. *J. Am. Chem. Soc.*, **127**, 3692–3693.
48. Hong,I.S., Ding,H. and Greenberg,M.M. (2006) Oxygen independent DNA interstrand cross-link formation by a nucleotide radical. *J. Am. Chem. Soc.*, **128**, 485–491.
49. Lee,Y.A., Yun,B.H., Kim,S.K., Margolin,Y., Dedon,P.C., Geacintov,N.E. and Shafirovich,V. (2007) Mechanisms of guanine oxidation in DNA by carbonate radical anion, a decomposition product of nitrosoperoxycarbonate. *Chem. Eur. J.*, **13**, 4571–4581.
50. Pratviel,G. and Meunier,B. (2006) Guanine oxidation: one- and two-electron reactions. *Chem. Eur. J.*, **12**, 6018–6030.
51. Perrier,S., Hau,J., Gasparutto,D., Cadet,J., Favier,A. and Ravanat,J.L. (2006) Characterization of lysine-guanine cross-links upon one-electron oxidation of a guanine-containing oligonucleotide in the presence of a trilysine peptide. *J. Am. Chem. Soc.*, **128**, 5703–5710.
52. Hildenbrand,K. (1990) The $SO_4^{\bullet-}$-induced oxidation of 2′-deoxyuridine-5′-phosphate, uridine-5′-phosphate and thymidine-5′-phosphate - an ESR study in aqueous-solution. *Z. Naturforsch, Teil C*, **45**, 47–58.
53. Shaw,A.A. and Cadet,J. (1990) Radical combination processes under the direct effects of gamma radiation on thymidine. *J. Chem. Soc. Perkin Trans.*, **2**, 2063–2070.
54. Steenken,S., Jovanovic,S.V., Bietti,M. and Bernhard,K. (2000) The trap depth (in DNA) of 8-oxo-7,8-dihydro-2′deoxyguanosine as derived from electron-transfer equilibria in aqueous solution. *J. Am. Chem. Soc.*, **122**, 2373–2374.
55. Lu,C., Lin,W., Wang,W., Han,Z., Yao,S. and Lin,N. (2000) Riboflavin (VB2) photosensitized oxidation of 2′-deoxyguanosine-5′-monophosphate (dGMP) in aqueous solution: a transient intermediates study. *Phys. Chem. Chem. Phys.*, **2**, 329–334.
56. Cadet,J., Berger,M., Buchko,G.W., Joshi,P.C., Raoul,S. and Ravanat,J.-L. (1994) 2,2-Diamino-4-[(3,5-di-*O*-acetyl-2-deoxy-β-D-*erythro*- pentofuranosyl)amino]-5-(2*H*)-oxazolone: A novel and predominant radical oxidation product of 3′,5′-di-*O*-acetyl-2′-deoxyguanosine. *J. Am. Chem. Soc.*, **116**, 7403–7404.
57. Kino,K., Saito,I. and Sugiyama,H. (1998) Product analysis of GG-specific photooxidation of DNA via electron transfer: 2-Aminoimidazolone as a major guanine oxidation product. *J. Am. Chem. Soc.*, **120**, 7373–7374.
58. Deeble,D.J., Schluchmann,M.N., Steenken,S. and von Sonntag,C. (1990) Direct evidence for the formation of thymine radical cations from the reaction of $SO_4^{\bullet-}$ with thymine derivatives: a pulse radiolysis study with optical and conductance detection. *J. Phys. Chem.*, **94**, 8186–8192.
59. Aravindakumar,C.T., Schluchmann,M.N., Rao,B.S.M., von Sonntag,J. and von Sonntag,C. (2003) The reactions of cytidine and 2′-deoxycytidine with $SO_4^{\bullet-}$ revisited. Pulse radiolysis and product studies. *Org. Biomol. Chem.*, **1**, 401–408.